Journal of Systems Engineering and Electronics
Vol. 30, No. 4, August 2019, pp.749 – 759

Retrieval strategy for failed satellite on tether's optimal balance swing angle

HAN Yanhua* and HONG Junting

College of Astronautics, Nanjing University of Aeronautics and Astronautics, Nanjing 210016, China

Abstract: A retrieval control strategy for failed satellite, which is connected to a servicing spacecraft by a tether, is studied. The Lagrange analytical mechanics based dynamics modeling for the system composed of a servicing spacecraft, a tether and a failed satellite, is presented under the earth center inertia coordinate system, then model simplification is conducted under the assumption that the failed satellite's mass is far smaller than the servicing spacecraft's, meanwhile the tether's length is far smaller than the size of the servicing spacecraft's orbit. Analysis shows that the retrieval process is intrinsically unstable as the Coriolis force functions is a negative damping. A retrieval strategy based on only the tether's tension is designed, resulting in the fastest retrieval speed. In the proposed strategy, firstly, the tether's swing angle amplitude is adjusted to 45° by deploying/retrieving the tether; then the tether swings freely with fixed length until it reaches negative maximum angle −45°; finally, the tether is retrieved by the pre-assigned exponential law. For simplicity, only the coplanar situation, that the tether swings in the plane of the servicing spacecraft's orbit, is studied. Numerical simulation verifies the effectiveness of the strategy proposed.

Keywords: tethered space tug (TST), retrieval control strategy, failed satellite, space debris, on-orbit service.

DOI: 10.21629/JSEE.2019.04.12

1. Introduction

Now space debris is regarded as a serious problem for space operational missions since the number of satellites in the earth orbit is steadily increasing. Therefore, effective measures to remove the debris are becoming urgent [1].

The electro-dynamic tether (EDT) technology, due to its high efficiency of orbital transfer and low demand for propellant, attracts scientists' and engineers' attention in the space debris active removal field [2]. Wen et al. [3] presented a nonlinear optimal control scheme for the three-dimensional retrieval process of an electro-dynamic tethered satellite system in an inclined orbit. The simulation results show that the control action is carried out by only adjusting the tensional and electro-dynamic forces in the tether. Wen et al. [4] presented a model predictive control (MPC) scheme for the retrieval of an electro dynamic tethered sub-satellite in an inclined orbit. The control action is realized by adjusting only the tensional and electrodynamic forces in the tether. In [5], a simple but nonsingular formulation was proposed for modeling the attitude dynamics of an EDT system based on the dumbbell assumption. Instead of the conventional means using two angular parameters, a unit vector along the EDT is taken to define the orientation of it, such that the singularities in the dynamic equations can be avoided.

Tethered space robot (TSR) or tethered space tug (TST), consisting of a space robot, a space tether, and a space platform/tug, is a promising technology for on-orbit servicing due to its flexibility and wide operation range [6,7]. Huang et al. [8] established the impact dynamic model for target capturing and presented an adaptive robust controller to achieve target capturing by TSR. Huang et al. [9] also presented a robust adaptive back-stepping controller to achieve stabilization of a tumbling tethered space robot-target combination. In [10], the attitude motion of debris during tethered towing was investigated, and the study revealed that, for safety reasons, elastic tethers should be avoided because they can lead to target attitude motion excitation and thus debris collision and fragmentation. In [11,12], an adaptive retrieval control law of the combination composed of TSR and target satellite, considering the combination's parameters uncertainties was presented. Lakso et al. [13] presented an approach to determine optimal tether deployment/retrieval trajectories using direct collocation and nonlinear programming. Lyapunov based deployment and retrieval control strategy resulting in the asymptotic stability was proposed in [14], then to optimize the effects of retrieval control, the partitioning and segmenting strategies on the orbit were proposed. In [15,16],

Manuscript received February 27, 2018.
*Corresponding author.
This work was supported by the Fundamental Research Funds for the Central Universities (NUAA_NS2016082).

that such criteria as minimum tension or minimum libration angles are inappropriate for defining the tethered satellite deployment/retrieval reference trajectories was demonstrated. By applying various optimality criteria, such as minimum tension rate, minimum length acceleration, as well as mini-max optimal control techniques, it is shown that the best control objectives should incorporate the minimization of system accelerations. With the timescale separation method, Zhong et al. [17] developed a computationally efficient algorithm with an acceptable accuracy to solve an optimal-control problem of TST systems during the propulsion stage of a Hohmann transfer that removes space debris from a geostationary orbit to the graveyard orbit. What is particularly worth mentioning is [18], in which, a new fractional order tension control law was proposed. Unlike the existing memoryless integer order control laws based on the feedback of the current state, the proposed fractional order control law has the memory of previous states and thus controls the tether retrieval more smoothly while maintaining the retrieving speed. Yu et al. [19] showed that the J2 perturbation and heating flux's effect on the tethered system should be paid sufficient attention since it has a significant impact on dynamics and control during the tethered system's retrieval process. In [20], a novel concept, the double-tethered space-tug, was proposed, then the dynamics and control of the system were discussed.

Compared with TSR or TST, the tethered space net (TSN) has a very large envelope area, and it can be applied to arbitrary space debris, so it has attracted more and more attention of researchers for the operation of the uncooperative space target. In [21,22], a new concept named maneuverable TSN (MTSN) used for uncooperative space target capture and removal was proposed. The MTSN inherits the maneuverability and the long working range from the TSR, and then the easy capture from the TSN. Different from the traditional TSN, position and configuration of the MTSN is controllable via four maneuvering units (MUs) located at four corners of a square net, which can be understood as four micro-satellites. In [23], an adaptive robust formation control strategy for the constrained multi-agent system was proposed, then the strategy was applied to the TSN robot (TSNR) for the maintenance of the easy-capture configuration while enabling the relative distance constraint between MUs during the space net approaching target phase. Based on the Hamilton principle, a novel dynamics model which revealed distinctive velocity jump phenomenon and a corresponding controller was proposed in [24] to resolve the approach control problem of MTSN. Based on the contact dynamics of rigid robots and the extended Hamilton's principle, Huang et al. [25] presented a novel dynamics modeling method for this new rigid-flexible coupling system for MTSN.

As for other novel ways of removing on-orbit debris, Castronuovo [26] envisaged the launch of a satellite carrying a number of de-orbiting devices, such as solid propellant kits. The satellite performs a rendezvous with an identified object and mates with it by means of a robotic arm. A de-orbiting device is attached to the object by means of a second robotic arm, then the object is released and the device is activated. The spacecraft travels then to the next target. Pascal et al. [27] presented a novel retrieval mode named "crawls", in which the tether was deployed previously from a space station, then the sub-satellite crawled along the tether rather than be retrieved by the tether toward the space station as used in the traditional form. In [28,29], a debris removal scheme, in which a spinning satellite captured and ejected debris, exploiting the impulsive momentum exchanges in place of fuel was reported. Ejected debris is sent to lower perigee orbits, or to re-enter the atmosphere.

For a failed satellite, capturing and retrieving it is perhaps a preferable choice, as the retrieved satellite may be repaired, then used again, or the expensive components and propellant on it can be torn down or exhausted out for reutilization. Retrieval of the satellite by the tether is a promising method in the future.

In comparison to the deployment control, the challenge of retrieval control comes from the intrinsical instability of its dynamics. From the aforementioned, we see that most retrieval processes need TSR's jet force or the tether's electro-dynamic force auxiliary control except for the tether's tensional control. Both TSR's jet force and the tether's electrodynamic force need an auxiliary device. For example, the former needs a jet engine, while the latter needs an electron release/collection device. Thus the system complexity is increased inevitably. Especially, for the robot's jet force auxiliary control, the valuable propellant is necessarily consumed. What is more, some retrieval control designs bring into the assumption of tether's small swing angle linearization, so in the situation of a big swing angle, the stability of the closed-loop cannot be guaranteed, so the range of application of the control method is inevitably narrowed. As for optimal retrieval control methods, most of them are solved by discretization and subsequent nonlinear programming. It is well known that the method of nonlinear programming is time-consuming, and cannot guarantee the convergence within the optimal solution. Adaptive and MPC based retrieval control can realize stability of the closed-loop, yet the on-line computation burden is heavy, and the complexity of the algorithm makes it not to be accepted easily for engineers.

In this paper, a retrieval control strategy is proposed, which overcomes successfully the instability of the re-

trieval process by force balance subtly. In addition, neither the assumption of the small swing angle, nor the electrodynamic force and robot's jet force auxiliary control is needed. That is, the retrieval process can be realized only by the tension force of the tether. Meanwhile the control law is very simple mathematically to be implemented in engineering. Specifically speaking, the tether's in-plane swing angle will remain at an "optimal" trimmed value and the tether's retrieval rate varies in accordance with a preassigned exponential law, resulting in the fastest retrieval.

The dynamics model of the TST will be established using Lagrange analytical mechanics under the earth center inertia coordinate system. Research effort will focus on the retrieval control strategy only by the tether's tension or the retrieval rate.

The rest of this paper is organized as follows. Section 1 establishes the system dynamics model. The stability of the retrieval process is analyzed in Section 2. Then retrieval control strategy is presented in Section 3. In Section 4, numerical simulation is given to verify the effectiveness of the presented control strategy. Finally, Section 5 concludes this paper.

2. System dynamics modeling

The tethered system is composed of a servicing spacecraft, a tether, and a failed satellite as shown in Fig. 1.

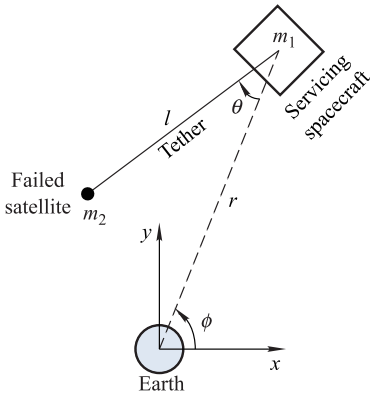

Fig. 1 Sketch of tethered system in orbit plane

The mass of the servicing spacecraft and the failed satellite, connected by an inelastic tether with the length l, are m_1 and m_2, respectively. r and ϕ denote the distance and phase angle of the servicing spacecraft with respect to the center of Earth, respectively. θ denotes the in-plane swing angle of the tether. Axis x points at a fixed direction in the inertia space. Axis y is got by rotating axis x with 90° anticlockwise. During the free swing stage (the tether's length is fixed), the generalized coordinates vector is defined as $\boldsymbol{q} \triangleq (r, \phi, \theta)^{\mathsf{T}}$, and the corresponding generalized force vector is $\boldsymbol{Q} = (0, 0, 0)^{\mathsf{T}}$ considering that the tension N of the tether is an ideal constraint force. During the tether deployment/retrieval stage (the tether's length is time-variant), the generalized coordinates vector is defined as $\boldsymbol{q} \triangleq (r, \phi, l, \theta)^{\mathsf{T}}$, and the corresponding generalized force vector is $\boldsymbol{Q} = (0, 0, N, 0)^{\mathsf{T}}$ considering that the tension N of the tether is an active force. Defining $\mu = GM_{\mathrm{e}}$, where G and M_{e} are the gravitational constant, the mass of Earth, respectively. Then the kinetic energy and gravitational potential energy of the servicing spacecraft and the failed satellite T_1, T_2, V_1 and V_2 can be calculated as follows:

$$\begin{cases} T_1 = \dfrac{1}{2} m_1 (\dot{r}^2 + r^2 \dot{\phi}^2) \\ T_2 = \dfrac{1}{2} m_2 \{[\dot{r}\sin\phi + r\dot{\phi}\cos\phi - \dot{l}\sin(\phi-\theta) - \\ \qquad l(\dot{\phi}-\dot{\theta})\cos(\phi-\theta)]^2 + [\dot{r}\cos\phi - r\dot{\phi}\sin\phi - \\ \qquad \dot{l}\cos(\phi-\theta) + l(\dot{\phi}-\dot{\theta})\sin(\phi-\theta)]^2\} \\ V_1 = -\dfrac{\mu m_1}{r} \\ V_2 = -\dfrac{\mu m_2}{\sqrt{l^2 + r^2 - 2lr\cos\theta}} \end{cases} . \tag{1}$$

Lagrangian function is

$$L = T_1 + T_2 - V_1 - V_2. \tag{2}$$

Substituting (1) and (2) into the second Lagrange equation

$$\left(\frac{\mathrm{d}}{\mathrm{d}t}\frac{\partial}{\partial \dot{\boldsymbol{q}}} - \frac{\partial}{\partial \boldsymbol{q}}\right) L = \boldsymbol{Q} \tag{3}$$

yields the system dynamics equations as follows.

For the stage of free swing,

$$\begin{cases} \ddot{r} = \dfrac{-\mu}{(m_1+m_2)r^2}(m_1 + m_2\sin^2\theta) + \\ \qquad \dfrac{\mu m_2 (l - r\cos\theta)\cos\theta}{(m_1+m_2)\sqrt{l^2 - 2lr\cos\theta + r^2}^3} + \\ \qquad \dfrac{1}{m_1+m_2}\{[m_1 r + m_2(r - l\cos\theta)]\dot{\phi}^2 - \\ \qquad m_2 l\dot{\theta}^2\cos\theta + 2m_2 l\dot{\phi}\dot{\theta}\cos\theta\} \\ \ddot{\phi} = \dfrac{1}{(m_1+m_2)r}[m_2 l(\dot{\phi}-\dot{\theta})^2\sin\theta - \\ \qquad 2(m_1+m_2)\dot{r}\dot{\phi} + \\ \qquad \mu m_2\left(\dfrac{r\cos\theta - l}{\sqrt{l^2 - 2lr\cos\theta + r^2}^3} - \dfrac{\cos\theta}{r^2}\right)\sin\theta] \\ \ddot{\theta} = \dfrac{\mu[m_2 l(r\cos\theta - l) - (m_1+m_2)r^2]}{(m_1+m_2)lr\sqrt{l^2 - 2lr\cos\theta + r^2}^3}\sin\theta + \\ \qquad \dfrac{1}{lr^2}(\mu\sin\theta - 2lr\dot{r}\dot{\phi}) + \\ \qquad \dfrac{m_2[lr^2(\dot{\phi}-\dot{\theta})^2 - \mu\cos\theta]}{(m_1+m_2)r^3}\sin\theta \end{cases} . \tag{4}$$

The tension of the tether can be calculated as follows according to Newton's Second Law with respect to m_1.

$$N=\frac{m_1m_2}{m_1+m_2}[l(\dot{\phi}-\dot{\theta})^2+\mu(\frac{r\cos\theta-l}{\sqrt{l^2-2lr\cos\theta+r^2}^3}-\frac{\cos\theta}{r^2})] \tag{5}$$

For the stage of deployment/retrieval,

$$\begin{cases}\ddot{r}=-\dfrac{\mu}{r^2}+r\dot{\phi}^2-\dfrac{N\cos\theta}{m_1}\\ \ddot{\phi}=-\dfrac{2\dot{r}\dot{\phi}}{r}+\dfrac{N\sin\theta}{m_1r}\\ \ddot{l}=\mu(\dfrac{r\cos\theta-l}{\sqrt{l^2-2lr\cos\theta+r^2}^3}-\dfrac{\cos\theta}{r^2})+l(\dot{\phi}-\dot{\theta})^2-\dfrac{m_1+m_2}{m_1m_2}N\\ \ddot{\theta}=\dfrac{\mu\sin\theta}{l}(\dfrac{1}{r^2}-\dfrac{r}{\sqrt{l^2-2lr\cos\theta+r^2}^3})-\dfrac{2\dot{r}\dot{\phi}}{r}+\dfrac{2\dot{l}}{l}(\dot{\phi}-\dot{\theta})+\dfrac{N\sin\theta}{m_1r}\end{cases}. \tag{6}$$

Defining the mass scale $\overline{m}\triangleq m_2$, the length scale $\overline{l}\triangleq r_0$ (the initial value of r), then deducing the time scale $\overline{t}\triangleq 2\pi\sqrt{\dfrac{\overline{l}^3}{\mu}}$ and the force scale $\overline{F}\triangleq \overline{m}\overline{l}/\overline{t}^2$, the dimensionless mass, length, time and force can be obtained as shown in Table 1.

The following dimensionless equations can be obtained according to (4)–(6) and Table 1.

Table 1 Dimensionless variables and/or parameters

Dimensionless variables and/or parameters	Computational formula
Dimensionless mass	$m_1^*=\dfrac{m_1}{\overline{m}}\triangleq\dfrac{1}{\varepsilon}$ $\quad m_2^*=\dfrac{m_2}{\overline{m}}=1$
Dimensionless length	$r^*=\dfrac{r}{\overline{l}}$ $\quad l^*=\dfrac{l}{\overline{l}}$
Dimensionless time	$t^*=\dfrac{t}{\overline{t}}$
Dimensionless force	$N^*=\dfrac{N}{\overline{F}}$

For the stage of free swing,

$$\begin{cases}r^{*\prime\prime}=\dfrac{-4\pi^2}{(1+\varepsilon)r^{*2}}(1+\varepsilon\sin^2\theta)+\dfrac{4\pi^2\varepsilon(l^*-r^*\cos\theta)\cos\theta}{(1+\varepsilon)\sqrt{l^{*2}-2l^*r^*\cos\theta+r^{*2}}^3}+\dfrac{1}{(1+\varepsilon)}\{[(1+\varepsilon)r^*-\varepsilon l^*\cos\theta]\phi'^2-\\ \quad\varepsilon l^*\theta'^2\cos\theta+2\varepsilon l^*\phi'\theta'\cos\theta\}\\ \phi''=\dfrac{1}{(1+\varepsilon)r^*}[\varepsilon l^*(\phi'-\theta')^2\sin\theta-2(1+\varepsilon)r^{*\prime}\phi'+4\pi^2\varepsilon(\dfrac{r^*\cos\theta-l^*}{\sqrt{l^{*2}-2l^*r^*\cos\theta+r^{*2}}^3}-\dfrac{\cos\theta}{r^{*2}})\sin\theta]\\ \theta''=4\pi^2\dfrac{[\varepsilon l^*(r^*\cos\theta-l^*)-(1+\varepsilon)r^{*2}]\sin\theta}{(1+\varepsilon)l^*r^*\sqrt{l^{*2}-2l^*r^*\cos\theta+r^{*2}}^3}+\dfrac{2}{l^*r^{*2}}(2\pi^2\sin\theta-l^*r^*r^{*\prime}\phi')+\\ \quad\dfrac{\varepsilon\sin\theta}{(1+\varepsilon)r^{*3}}[l^*r^{*2}(\phi'-\theta')^2-4\pi^2\cos\theta]\end{cases} \tag{7}$$

$$N^*=\frac{1}{(1+\varepsilon)}[l^*(\phi'-\theta')^2+4\pi^2(\frac{r^*\cos\theta-l^*}{\sqrt{l^{*2}-2l^*r^*\cos\theta+r^{*2}}^3}-\frac{\cos\theta}{r^{*2}})]. \tag{8}$$

For the stage of deployment/retrieval,

$$\begin{cases}r^{*\prime\prime}=-\dfrac{4\pi^2}{r^{*2}}+r^*\phi'^2-\varepsilon N^*\cos\theta\\ \phi''=-\dfrac{2r^{*\prime}\phi'}{r^*}+\dfrac{\varepsilon N^*\sin\theta}{r^*}\\ l^{*\prime\prime}=\dfrac{-4\pi^2\cos\theta}{r^{*2}}+\dfrac{4\pi^2(r^*\cos\theta-l^*)}{\sqrt{l^{*2}-2l^*r^*\cos\theta+r^{*2}}^3}+l^*(\phi'-\theta')^2-(1+\varepsilon)N^*\\ \theta''=\dfrac{4\pi^2\sin\theta}{l^*r^{*2}}-\dfrac{4\pi^2r^*\sin\theta}{l^*\sqrt{l^{*2}-2l^*r^*\cos\theta+r^{*2}}^3}-\dfrac{2r^{*\prime}\phi'}{r^*}+\dfrac{2l^{*\prime}(\phi'-\theta')}{l^*}+\dfrac{\varepsilon N^*\sin\theta}{r^*}\end{cases} \tag{9}$$

where the prime "′" and "″" denote the first and second order derivatives with respect to dimensionless time "t^*", respectively.

Assuming that the mass of the failed satellite is far less than that of the servicing spacecraft, namely $m_2 \ll m_1$, then $0 < \varepsilon \ll 1$, and the length of the tether is far less than the size of the orbit of the servicing spacecraft, namely $l^* \ll r^*$, then (7)–(9) can be simplified as follows.

For both stages of free swing and deployment/retrieval,

$$\begin{cases} r^{*\prime\prime} = -\dfrac{4\pi^2}{r^{*2}} + r^*\phi'^2 \\ \phi'' = \dfrac{-2r^{*\prime}\phi'}{r^*} \end{cases}. \tag{10}$$

For the stage of free swing,

$$\begin{cases} \theta'' = -\dfrac{6\pi^2 \sin 2\theta}{r^{*3}} - \dfrac{2r^{*\prime}\phi'}{r^*} \\ N^* = l^*[(\phi' - \theta')^2 + \dfrac{4\pi^2}{r^{*3}}(3\cos^2\theta - 1)] \end{cases}. \tag{11}$$

For the stage of deployment/retrieval,

$$\begin{cases} l^{*\prime\prime} = l^*[\dfrac{4\pi^2}{r^{*3}}(3\cos^2\theta - 1) + (\phi' - \theta')^2] - N^* \\ \theta'' = -\dfrac{6\pi^2 \sin 2\theta}{r^{*3}} - \dfrac{2r^{*\prime}\phi'}{r^*} + \dfrac{2l^{*\prime}(\phi' - \theta')}{l^*} \end{cases}. \tag{12}$$

According to the orbit dynamics of a satellite, if the initial condition $(r_0, \dot{r}_0, \dot{\phi}_0)$ of the servicing spacecraft meets the following equation

$$e = \sqrt{1 + \frac{(r_0\dot{r}_0^2 + r_0^3\dot{\phi}_0^2 - 2\mu)r_0^3\dot{\phi}_0^2}{\mu^2}} = 0 \tag{13}$$

where e is the eccentricity of the servicing spacecraft's orbit, then the orbit is a perfect circle, so (10) can be easily integrated to obtain the following:

$$\begin{cases} r^* \equiv 1, \quad r^{*\prime} \equiv 0 \\ \phi' \equiv 2\pi, \quad \phi'' \equiv 0 \end{cases}. \tag{14}$$

Substituting (14) into (11) and (12) yields

$$\begin{cases} \theta'' = -6\pi^2 \sin 2\theta \\ N^* = l^*[(2\pi - \theta')^2 + 4\pi^2(3\cos^2\theta - 1)] \end{cases} \tag{15}$$

$$\begin{cases} l^{*\prime\prime} = l^*[4\pi^2(3\cos^2\theta - 1) + (2\pi - \theta')^2] - N^* \\ \theta'' = -6\pi^2 \sin 2\theta + \dfrac{2l^{*\prime}(2\pi - \theta')}{l^*} \end{cases}. \tag{16}$$

3. Stability analysis for tether retrieval process

The analytical solution of the first equation of (15) can be derived as follows [30]:

$$\theta = \arcsin[k \cdot \mathrm{sn}(2\sqrt{3}\pi t^*)] \tag{17}$$

where sn is an elliptic function.

$$k = \sin\theta_0 \tag{18}$$

where θ_0 is the initial value of the tether swing angle θ.

Equation (17) denotes a periodic function of t^*, with period as

$$T^* = \frac{2}{\sqrt{3}\pi}\mathrm{K}(k) = \frac{1}{\sqrt{3}}[1 + (\frac{1}{2})^2k^2 + (\frac{1}{2}\cdot\frac{3}{4})^2k^4 + (\frac{1}{2}\cdot\frac{3}{4}\cdot\frac{5}{6})^2k^6 + \cdots] \tag{19}$$

where K denotes the first complete elliptic integral [30].

It can be seen that the free swing of the tether is stable. Following that, we analyze the stability of the tether retrieval stage. For this purpose, we study the second equation of (16). The equation can be rewritten as follows:

$$\theta'' + \frac{2l^{*\prime}}{l^*}\theta' + 6\pi^2 \sin 2\theta = \frac{4\pi l^{*\prime}}{l^*}. \tag{20}$$

The second term $\dfrac{2l^{*\prime}}{l^*}\theta'$ on the left side of the equation is the Coriolis force induced by the tether's length rate $l^{*\prime}$ and the swing angle rate θ' together, functioning as a damping force. The third term $6\pi^2 \sin 2\theta$ on the left side of the equation functions as a restoring force. The term $\dfrac{4\pi l^{*\prime}}{l^*}$ on the right side of the equation is the Coriolis force induced by the tether's length rate $l^{*\prime}$ and the whole combined system's orbit angular velocity 2π together, functioning as an external drive input.

The length rate of the tether during retrieval stage is negative, that is $l^{*\prime} < 0$, so the term $\dfrac{2l^{*\prime}}{l^*}\theta'$ in (20) is always a negative damping, resulting in the divergence of the swing angle θ, so we see that the retrieval process of tether is intrinsically unstable.

4. Retrieval control strategy

To guarantee that the variable θ not to diverge during tether retrieval stage, it is necessary that the damping term $\dfrac{2l^{*\prime}}{l^*}\theta'$ in (20) holds zero, namely that $\theta \equiv \widehat{\theta}(\mathrm{constant})$, $\theta' \equiv 0$, and $\theta'' \equiv 0$. Under this condition, (20) becomes

$$6\pi^2 \sin 2\widehat{\theta} = \frac{4\pi l^{*\prime}}{l^*}. \tag{21}$$

Thus,

$$l^{*\prime} = \frac{3}{2}\pi l^* \sin 2\widehat{\theta}. \tag{22}$$

We see that, if the tether's length begins to vary in accordance with the law described in (22) upon the moment

θ' reaching zero (namely the moment that θ reaches its maximum positive or negative value $\pm|\theta|_{\max}$), then the external drive force term $\dfrac{4\pi l^{*\prime}}{l^*}$ counteracts exactly the restoring term $6\pi^2\sin 2\theta$ in (20), resulting in that swing angle of the tether θ holds the constant value $\widehat{\theta}=|\theta|_{\max}$ or $\widehat{\theta}=-|\theta|_{\max}$ all the time afterward.

The analytical solution of (22) can be easily derived as follows:

$$l^*=l_0^*\mathrm{e}^{(\frac{3}{2}\pi\sin 2\widehat{\theta})t^*} \tag{23}$$

where l_0^* is the value of $l^*(t^*)$ at the initial time $t^*=0$.

Equation (23) indicates that the tether's length varies in accordance with the exponential law, and obviously, only when $\widehat{\theta}<0$ the length of the tether decreases. Thus, we see that the retrieval action should be taken at the moment that the tether's swing angle reaches its negative maximum value $-|\theta|_{\max}$. Additionally, we see that while $\widehat{\theta}=-|\theta|_{\max}=-\dfrac{\pi}{4}$, then $\sin 2\widehat{\theta}=-1$, so the length of the tether decreases at its full speed.

Let $l_{\min}^*$ denote the threshold value terminating the tether retrieval process, then according to (23), the consumed time of the retrieval process can be calculated easily as follows:

$$T^*=\frac{2}{3\pi\sin 2\widehat{\theta}}\ln\frac{l_{\min}^*}{l_0^*}. \tag{24}$$

Taking the first and second order derivatives, respectively, of (23) with respect to the dimensionless time t^* yields the dimensionless rate and acceleration of the tether's length as follows:

$$\begin{cases} l^{*\prime}=\dfrac{3}{2}\pi l_0^*\sin 2\widehat{\theta}\cdot\mathrm{e}^{(\frac{3}{2}\pi\sin 2\widehat{\theta})t^*} \\ l^{*\prime\prime}=\dfrac{9}{4}\pi^2 l_0^*\sin^2 2\widehat{\theta}\cdot\mathrm{e}^{(\frac{3}{2}\pi\sin 2\widehat{\theta})t^*} \end{cases}. \tag{25}$$

For the stage of the tether's free swing, its amplitude $|\widehat{\theta}|$ can be determined by the value of θ and θ' together at any moment according to the following formula:

$$|\widehat{\theta}|=\frac{1}{2}\arccos(\cos 2\theta-\frac{\theta'^2}{6\pi^2}). \tag{26}$$

Now we study the problem that if $|\widehat{\theta}|\neq\dfrac{\pi}{4}$, how we can regulate the tether's swing angle amplitude to the desired value $|\widehat{\theta}|=\dfrac{\pi}{4}$ only by deploying/retrieving the tether. Thus, we once again study (20). The equation can be transformed into

$$\theta''+6\pi^2\sin 2\theta=2\frac{l^{*\prime}}{l^*}(2\pi-\theta'). \tag{27}$$

Taking the term $2\dfrac{l^{*\prime}}{l^*}(2\pi-\theta')$ on the right side of (27) as the external drive force, we can see that, while the drive force denoted by the term is in the same direction as the tether swing, namely $\mathrm{sgn}[2\dfrac{l^{*\prime}}{l^*}(2\pi-\theta')]=\mathrm{sgn}\theta'$, the term does positive work to the tethered system, feeding energy into it, so the swing angle amplitude $|\theta|_{\max}$ will increase; otherwise, while $\mathrm{sgn}[2\dfrac{l^{*\prime}}{l^*}(2\pi-\theta')]=-\mathrm{sgn}\theta'$, the term does negative work, dissipating energy of the tethered system, so the swing angle amplitude $|\theta|_{\max}$ will decrease.

Obviously, $\mathrm{sgn}[2\dfrac{l^{*\prime}}{l^*}(2\pi-\theta')]=\mathrm{sgn}[l^{*\prime}(2\pi-\theta')]$ as $l^*>0$, meanwhile we notice the property of sign function that for the arbitrary real number a and b, there exists $\mathrm{sgn}a\cdot\mathrm{sgn}b=\mathrm{sgn}(ab)=\mathrm{sgn}(\dfrac{a}{b})=\mathrm{sgn}(\dfrac{b}{a})=\dfrac{\mathrm{sgn}a}{\mathrm{sgn}b}=\dfrac{\mathrm{sgn}b}{\mathrm{sgn}a}$, so the following conclusion can be drawn easily, that if

$$\mathrm{sgn}l^{*\prime}=\mathrm{sgn}\theta'\cdot\mathrm{sgn}(2\pi-\theta') \tag{28}$$

then the amplitude $|\theta|_{\max}$ will increase, else if

$$\mathrm{sgn}l^{*\prime}=-\mathrm{sgn}\theta'\cdot\mathrm{sgn}(2\pi-\theta') \tag{29}$$

the amplitude $|\theta|_{\max}$ will decrease.

According to (28) and (29), the following function curves of $l^{*\prime}$ with respect to θ' can be designed as shown in Fig. 2(a) and Fig. 2(b), respectively.

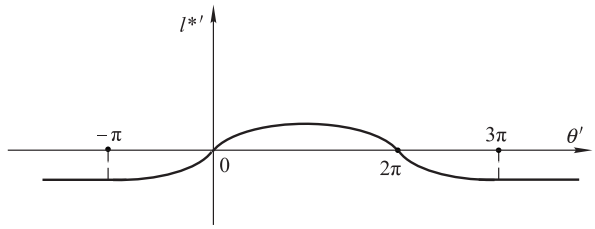

(a) Curves of $l^{*\prime}(\theta')$ according to (28) increase the swing amplitude of tether

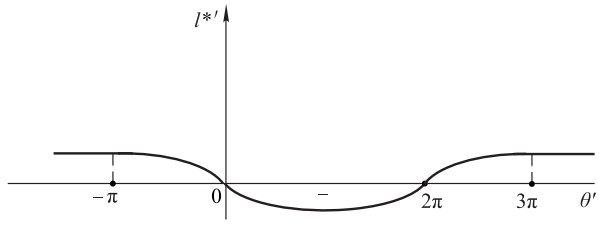

(b) Curves of $l^{*\prime}(\theta')$ according to (29) decrease the swing amplitude of tether

Fig. 2 Curves of $l^{*\prime}(\theta')$

The function formulas corresponding to the above curves are as follows.

To increase the amplitude $|\theta|_{\max}$,

$$l^{*\prime}=\begin{cases} l_{\max}^{*\prime}\sin(\dfrac{1}{2}\theta'), & -\pi\leqslant\theta'\leqslant 3\pi \\ -l_{\max}^{*\prime}, & \theta'<-\pi \text{ or } 3\pi<\theta' \end{cases}. \tag{30}$$

To decrease the amplitude $|\theta|_{\max}$,

$$l^{*\prime}=\begin{cases}-l^{*\prime}_{\max}\sin(\dfrac{1}{2}\theta'), & -\pi\leqslant\theta'\leqslant 3\pi\\ l^{*\prime}_{\max}, & \theta'<-\pi \text{ or } 3\pi<\theta'\end{cases}\tag{31}$$

where $l^{*\prime}_{\max}$ is the maximum rate which the tether can reach limited to the physical condition of the tether deployment/retrieval device amounted on the servicing spacecraft.

Taking the derivative of (30) and (31) with respect to the dimensionless time t^*, respectively, yields

$$l^{*\prime\prime}=\begin{cases}l^{*\prime}_{\max}[\dfrac{l^{*\prime}}{l^*}(2\pi-\theta')-3\pi^2\sin 2\theta]\cos(\dfrac{1}{2}\theta'), & \\ \quad -\pi\leqslant\theta'\leqslant 3\pi & \\ 0, \quad \theta'<-\pi \text{ or } 3\pi<\theta'\end{cases}\tag{32}$$

$$l^{*\prime\prime}=\begin{cases}-l^{*\prime}_{\max}[\dfrac{l^{*\prime}}{l^*}(2\pi-\theta')-3\pi^2\sin 2\theta]\cos(\dfrac{1}{2}\theta'), & \\ \quad -\pi\leqslant\theta'\leqslant 3\pi & \\ 0, \quad \theta'<-\pi \text{ or } 3\pi<\theta'\end{cases}.\tag{33}$$

The functions $l^{*\prime\prime}$ expressed in (32) and (33) are both continuous, guaranteeing the continuity of the tension force of the tether.

The formulas of the tension force of the tether can be calculated as follows according to (15) and (16).

For the stage of adjusting swing amplitude,

$$N^*=l^*[4\pi^2(3\cos^2\theta-1)+(2\pi-\theta')^2]-l^{*\prime\prime}.\tag{34}$$

For the stage of free swing,

$$N^*=l^*[4\pi^2(3\cos^2\theta-1)+(2\pi-\theta')^2].\tag{35}$$

For the stage of retrieving tether,

$$N^*=l^*[4\pi^2(3\cos^2\widehat{\theta}-1)+4\pi^2]-l^{*\prime\prime}\tag{36}$$

where $l^{*\prime\prime}$ in (34) can be calculated according to (32) and (33), while $l^{*\prime\prime}$ in (36) can be calculated according to (25). Finally, for the stage of retrieving tether,

$$N^*=3\pi^2 l_0^*(4-3\sin^2\widehat{\theta})\cos^2\widehat{\theta}\mathrm{e}^{(\frac{3}{2}\pi\sin 2\widehat{\theta})t^*}.\tag{37}$$

5. Numerical simulation

The input parameters for numerical simulation are shown in Table 2. In Table 2, R_{e} and h_0 denote, respectively, the radius of Earth and the initial distance of the servicing spacecraft from the surface of Earth.

Table 2 Input parameters for simulation

Input parameter	Value
$G/(\mathrm{m}^3\cdot\mathrm{kg}^{-1}\cdot\mathrm{s}^{-2})$	6.67×10^{-11}
M_{e}/kg	735×10^{20}
$\mu/(\mathrm{m}^3\cdot\mathrm{s}^{-2})$	3.99×10^{14}
R_{e}/km	6 371
m_1/kg	5 000
m_2/kg	200
h_0/km	400
r_0/km	6 771
ϕ_0	0
$\dot{\phi}_0/((^\circ)\cdot\mathrm{s}^{-1})$	0.064 5
l_0/m	1 000
$\dot{l}_{\max}/(\mathrm{m}\cdot\mathrm{s}^{-1})$	2
$l_{\min}$/m	1
$\theta_0/(^\circ)$	60
$\dot{\theta}_0$	0

The simulation results are shown in Figs. 3–9.

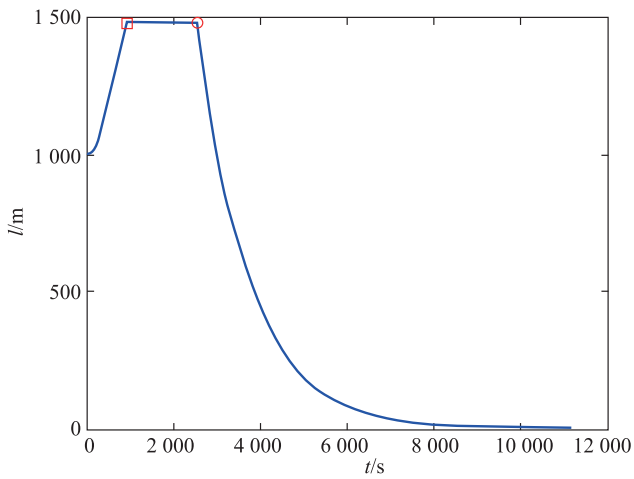

Fig. 3 Length of tether vs. time

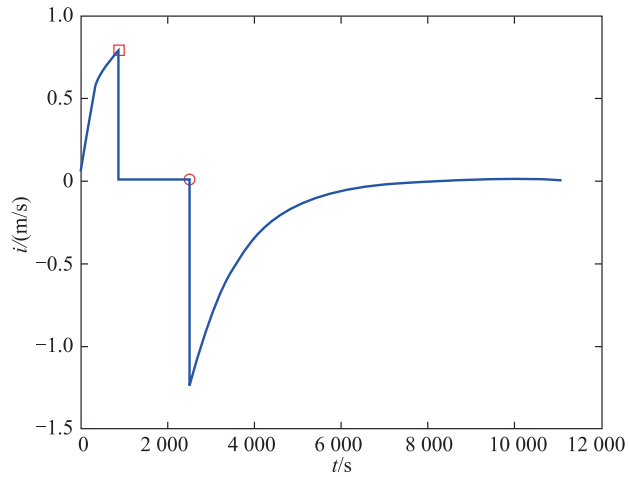

Fig. 4 Rate of tether's length vs. time

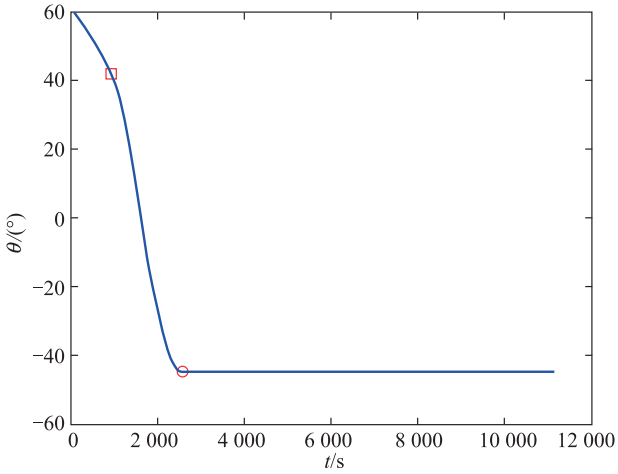

Fig. 5 Swing angle of tether vs. time

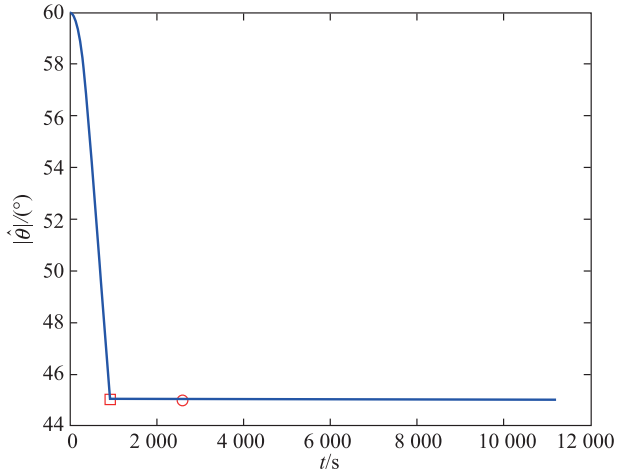

Fig. 6 Tether's swing amplitude vs. time determined by its swing angle and angle velocity

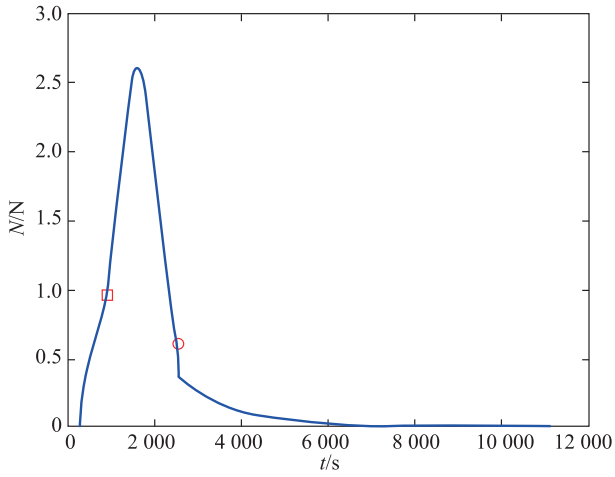

Fig. 7 The tension force of tether vs. time

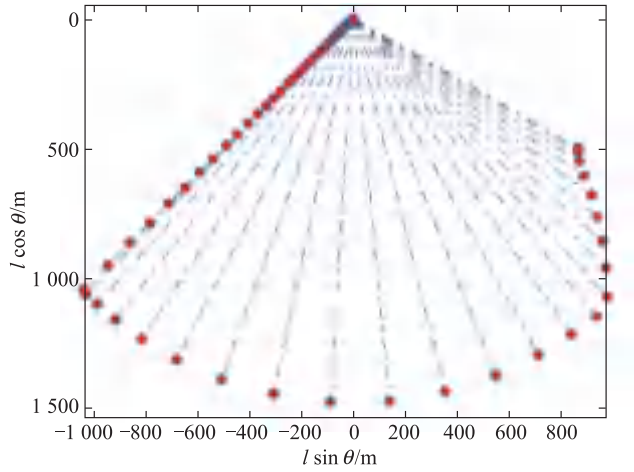

Fig. 8 Failed satellite's locus and tether's corresponding configuration under Cartesian coordinate system

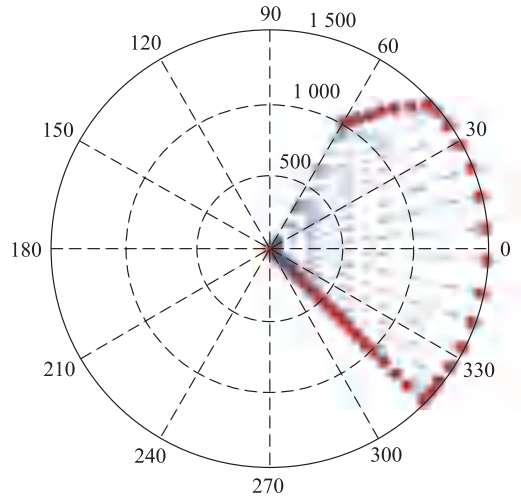

Fig. 9 Failed satellite's locus and tether's corresponding configuration under polar coordinate system

The whole retrieval stage is divided into three sub-stages: the first sub-stage is to adjust the tether's swing amplitude through deploying and/or retrieving the tether until the amplitude reaches the desired value $|\theta|_{\max} = 45°$; the second sub-stage is to let the tether swing freely with the fixed length until the swing angle reaches its negative maximum value, that is $\widehat{\theta} = -|\theta|_{\max} = -45°$; the third sub-stage is to retrieve the tether in accordance with the designed exponential law described in (23) until the tether's length decreases to the pre-assigned threshold value $l_{\min}$. In Figs. 3−7, the above three sub-stages are so identified by the red small boxes and small circles in each simulation result curves as: the curve prior to the red small box denotes the sub-stage of adjusting the swing amplitude; the curve between the red small box and small circle de-

notes the sub-stage of free swing; finally, the curve after the small circle denotes the sub-stage of retrieval.

In the scenario set for the simulation, the tether's swing amplitude is $60°$, different from the desired value $45°$, so we decrease the tether's swing amplitude by deploying the tether until the amplitude reaches $45°$ at time $t_1 = 926$ s, as shown in Fig. 5. Hereafter, the tether's length is fixed and the tether swing freely until its swing angle reaches the negative maximum value $\widehat{\theta} = -|\theta|_{\max} = -45°$ at time $t_2 = 2\ 549$ s. Then the tether's length is decreased in accordance with the pre-assigned exponential law, the swing angle remaining at $\widehat{\theta} = -|\theta|_{\max} = -45°$ because of the balance between the force $\dfrac{4\pi l^{*\prime}}{l^*}$ and the restoring force $6\pi^2 \sin 2\theta$ aforementioned, until the length of the tether reaches its threshold value $l_{\min} = 1$ m at time $t_3 = 11\ 185$ s. The consumed time $\Delta t = t_3 - t_2 = 8\ 636$ s in the retrieval sub-stage can be converted into the dimensionless time $\Delta t^* = \dfrac{\Delta t}{\bar{t}} = 1.548\ 0$, agreeing well with the estimated value according to (24).

Fig. 4 shows that the maximum value of the tether's length rate is $1.25\ \mathrm{m \cdot s^{-1}}$, not exceeding the pre-assigned value $\dot{l}_{\max} = 2\ \mathrm{m \cdot s^{-1}}$). Fig. 7 shows that the tension force of tether varies continuously during the whole retrieval process, while its maximum value is only 2.6 N, easily to implement in engineering practice.

Fig. 8 and Fig. 9 show intuitively the locus of the failed satellite (depicted by small red solid circles) and the tether's corresponding length and swing angle variations (depicted by blue dot dash line) during the whole retrieval stage. Fig. 8 is under the Cartesian coordinate system while Fig. 9 is under the polar coordinate system. The servicing spacecraft are in the center of the coordinate system in both figures.

For the same initial condition $l_0 = 1\ 000$ m, $\theta_0 = 60°$, $\dot{\theta}_0 = 0$, if the first sub-stage adjusting the swing angle amplitude through deploying/retrieving the tether is eliminated, the retrieval action begins directly with the second sub-stage which is the tether swinging freely with a fixed length, and when the swing angle reaches the negative maximum value $\widehat{\theta} = -60°$, the retrieval sub-stage starts. In the hypothetical scenario, the simulation results are shown in Figs. 10–13. In Fig. 10 and Fig. 11, the curves prior to the red small circle denote the sub-stage of free swing, while the curves after the red small circle denote the sub-stage of retrieval sub-stage. The simulation results show that the consumed time is $11\ 615$ s, longer than $11\ 185$ s in the strategy aforementioned with 430 s.

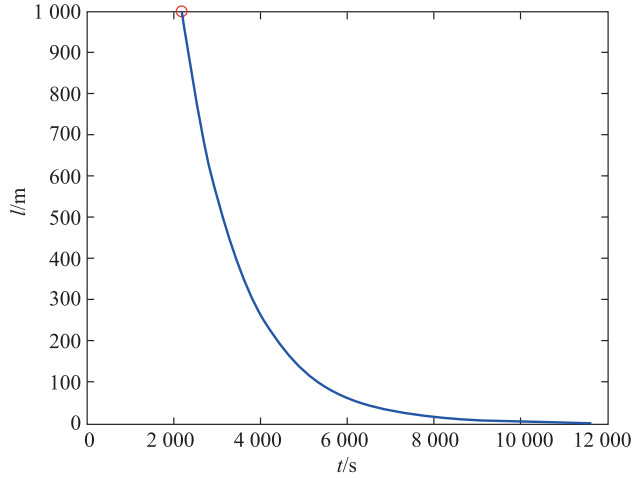

Fig. 10 Length of tether vs. time (without the sub-stage of adjusting the swing angle amplitude)

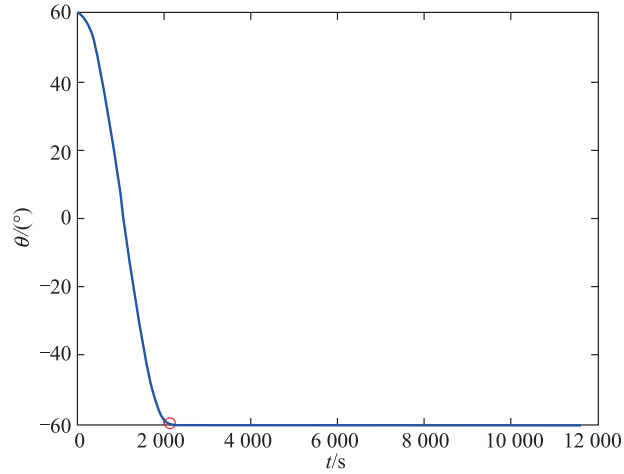

Fig. 11 Swing angle of tether vs. time (without the sub-stage of adjusting the swing angle amplitude)

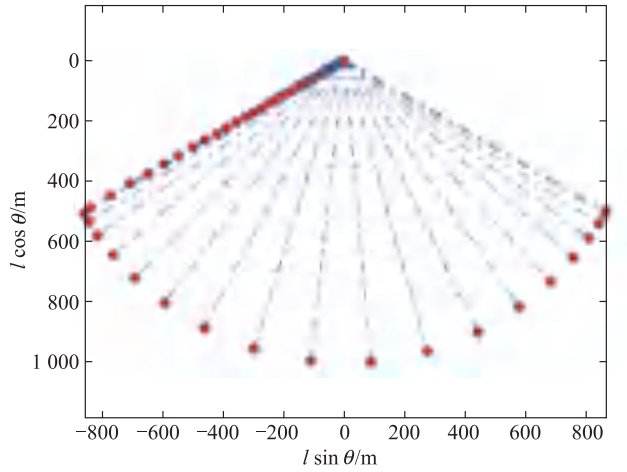

Fig. 12 Failed satellite's locus and tether's corresponding configuration under Cartesian coordinate system (without the sub-stage of adjusting the swing angle amplitude)

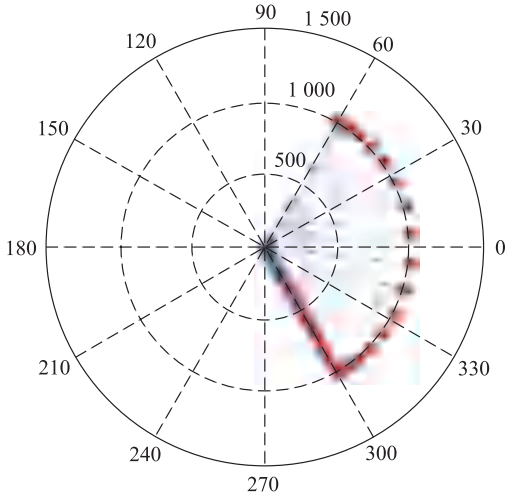

Fig. 13 Failed satellite's locus and tether's corresponding configuration under polar coordinate system (without the sub-stage of adjusting the swing angle amplitude)

6. Conclusions

The tethered system's in-plane dynamics modeling is presented and a retrieval strategy is designed in this paper aiming at the problem of failed satellite retrieval only by the tension of the tether connected to a servicing spacecraft. In the proposed strategy, firstly, the tether's swing angle amplitude is adjusted to 45° by only deploying/retrieving the tether; then the tether freely swing with a fixed length until it reaches negative maximum angle -45°; finally, the tether is retrieved by the pre-assigned exponential law. In the last retrieval sub-stage, the Coriolis force induced by the failed satellite's motion in the radial direction and the angular velocity of the whole tethered system together is balanced by the restoring force, so the tether's swing angle remains at -45°. The reason we choose the balanced swing angle as -45° is that the angle value will result in the fastest attenuation rate of the tether's length, being equivalent to the shortest time of retrieval. Simulation results have supported the effectiveness of the retrieval strategy proposed here.

Some assumptions are adopted in the dynamics modeling, e.g., the tether swings in the plane of servicing spacecraft's orbit, the mass of failed satellite is far smaller than that of servicing spacecraft, and the servicing spacecraft's orbit is a perfect circle. Additionally, the elasticity of the tether is not taken into consideration. The tether based retrieval strategy for the failed satellite or space debris under general conditions is the future work.

References

[1] SHAN M H, GUO J, JILL E. Review and comparison of active space debris capturing and removal methods. Progress in Aerospace Sciences, 2016, 80: 18 – 32.

[2] NISHIDA S I, KAWAMOTO S, OKAWA Y, et al. Space debris removal system using a small satellite. Acta Astronautica, 2009, 65: 95 – 102.

[3] WEN H, JIN D P, HU H Y. Retrieval control of an electrodynamic tethered satellite in an inclined orbit. Chinese Journal of Theoretical and Applied Mechanics, 2008, 40(3): 375 – 380. (in Chinese)

[4] WEN H, JIN D P, HU H Y. Feedback control for retrieving an electro-dynamic tethered sub-satellite. Tsinghua Science and Technology, 2009, 14(S2): 79 – 83.

[5] WEN H, JIN D P, HU H Y. Removing singularity of orientation description for modeling and controlling an electro-dynamic tether. Journal of Guidance, Control, and Dynamics, 2018, 41(3): 761 – 766.

[6] HUANG P F, HU Z H, MENG Z J. Coupling dynamics modeling and optimal coordinated control of tethered space robot. Aerospace Science and Technology, 2015, 41: 36 – 46.

[7] LINSKENS H T K, MOOIJ E. Tether dynamics analysis and guidance and control design for active space-debris removal. Journal of Guidance, Control, and Dynamics, 2016, 39(6): 1232 – 1243.

[8] HUANG P F, WANG D K, MENG Z J, et al. Impact dynamic modeling and adaptive target capturing control for tethered space robots with uncertainties. IEEE/ASME Trans. on Mechatronics, 2016, 21(5): 2260 – 2271.

[9] HUANG P F, WANG D K, MENG Z J, et al. Adaptive post-capture back-stepping control for tumbling tethered space robot – target combination. Journal of Guidance, Control, and Dynamics, 2016, 39(1): 150 – 156.

[10] JAWORSKI P, LAPPAS V, TSOURDOS A, et al. Debris rotation analysis during tethered towing for active debris removal. Journal of Guidance, Control, and Dynamics, 2017, 40(7): 1768 – 1778.

[11] MENG Z J, HUANG P F, WANG D K. In-plane adaptive retrieval method for tethered space robots after target capturing. Acta Aeronautica et Astronautica Sinica, 2015, 36(12): 4035 – 4042. (in Chinese)

[12] HUANG P F, ZHANG F, MENG Z J. Adaptive control for space debris removal with uncertain kinematics, dynamics and states. Acta Astronautica, 2016, 128: 416 – 430.

[13] LAKSO J J, COVERSTONE V L. Optimal tether deployment/retrieval trajectories using direct collocation. Proc. of the AIAA/AAS Astrodynamics Specialist Conference, 2000: 1 – 9.

[14] YU B S, JIN D P. Asymptotic stabilization for deployment and retrieval of a tethered satellite system. Chinese Space Science and Technology, 2013(5): 35 – 43. (in Chinese)

[15] WILLIAMS P, TRIVAILO P. On the optimal deployment and retrieval of tethered satellites. Proc. of the 41st AIAA/ASME/SAE/ASEE Joint Propulsions Conference and Exhibit, 2005, DOI: 10.2514/6.2005-4291.

[16] WILLIAMS P. Optimal deployment/retrieval of tethered satellites. Journal of Spacecraft and Rockets, 2008, 45(2): 324 – 343.

[17] ZHONG R, ZHU Z H. Timescale separate optimal control of tethered space-tug systems for space-debris removal. Journal of Guidance, Control, and Dynamics, 2016, 39(11): 2539 – 2544.

[18] SUN G H, ZHU Z H. Fractional order tension control for stable and fast tethered satellite retrieval. Acta Astronautica, 2014, 104: 304 – 312.

[19] YU B S, JIN D P. Deployment and retrieval of tethered satellite system under J_2 perturbation and heating effect. Acta Astronautica, 2010, 67: 845 – 853.

[20] QI R, MISRA A K, ZUO Z Y. Active debris removal using

double-tethered space-tug system. Journal of Guidance, Control, and Dynamics, 2017, 40(3): 720 – 728.
[21] ZHANG F, HUANG P F. Releasing dynamics and stability control of maneuverable tethered space net. IEEE/ASME Trans. on Mechatronics, 2017, 22(2): 983 – 993.
[22] ZHANG F, HUANG P F, MENG Z J, et al. Dynamics analysis and controller design for maneuverable tethered space net robot. Journal of Guidance, Control, and Dynamics, 2017, 40(11): 2828 – 2843.
[23] LIU Y, HUANG P F, ZHANG F, et al. Distributed formation control using artificial potentials and neural network for Constrained multi-agent systems. IEEE Trans. on Control Systems Technology, 2018. DOI: 10.1109/TCST.2018.2884226.
[24] MENG Z J, HUANG P F, GUO J. Approach modeling and control of an autonomous maneuverable space net. IEEE Trans. on Aerospace and Electronic Systems, 2017, 53(6): 2651 – 2661.
[25] HUANG P F, HU Z H, ZHANG F. Dynamic modeling and coordinated controller designing for the maneuverable tether-net space robot system. Multi-body System Dynamics, 2016, 36: 115 – 141.
[26] CASTRONUOVO M M. Active space debris removal — a preliminary mission analysis and design. Acta Astronautica, 2011, 69: 848-859.
[27] PASCAL M, DJEBLI A, BAKKALI L E. Laws of deployment/retrieval in tether connected satellites systems. Acta Astronautica, 1999, 45(2): 61-73.
[28] MISSEL J, MORTARI D. Path optimization for space sweeper with sling-sat: a method of active space debris removal. Advances in Space Research, 2013, 52: 1339-1348.
[29] MISSEL J, MORTARI D. Removing space debris through sequential captures and ejections. Journal of Guidance, Control, and Dynamics, 2013, 36(3): 743 – 752.
[30] ZEIDLER E, HACKBUSCH W, SCHWARZ H R, et al. Teubner-Taschenbuch der mathematik. LI W L. Trans. Beijing: Science Press, 2012. (in Chinese)

Biographies

HAN Yanhua was born in 1976. He received his Ph.D. degree in navigation, guidance and control from Northwestern Polytechnical University in 2006. He is currently an associate professor in the College of Astronautics at Nanjing University of Aeronautics and Astronautics. His research interests include tethered satellite system, and space manipulator.
E-mail: hanyanhua@nuaa.edu.cn

HONG Junting was born in 1993. She received her B.E. degree in building electrical and intelligent engineering from Sanjiang College in 2018. She is currently a graduate student in the College of Astronautics at Nanjing University of Aeronautics and Astronautics. Her research direction is system simulation.
E-mail: 1097524513@qq.com